

Green Chemistry

Accepted Manuscript



This is an *Accepted Manuscript*, which has been through the Royal Society of Chemistry peer review process and has been accepted for publication.

Accepted Manuscripts are published online shortly after acceptance, before technical editing, formatting and proof reading. Using this free service, authors can make their results available to the community, in citable form, before we publish the edited article. We will replace this *Accepted Manuscript* with the edited and formatted *Advance Article* as soon as it is available.

You can find more information about *Accepted Manuscripts* in the [Information for Authors](#).

Please note that technical editing may introduce minor changes to the text and/or graphics, which may alter content. The journal's standard [Terms & Conditions](#) and the [Ethical guidelines](#) still apply. In no event shall the Royal Society of Chemistry be held responsible for any errors or omissions in this *Accepted Manuscript* or any consequences arising from the use of any information it contains.



www.rsc.org/greenchem



Weighing the factors behind enzymatic hydrolyzability of pretreated lignocellulose

Ville Pihlajaniemi^a, Mika Henrikki Sipponen^a, Henrikki Liimatainen^b, Juho Antti Sirviö^b, Antti Nyssölä^a, Simo Laakso^a

Received 00th January 20xx,
Accepted 00th January 20xx

DOI: 10.1039/x0xx00000x

www.rsc.org/

The major factors determining enzymatic hydrolyzability of pretreated wheat straw were analyzed and their relative importance quantified. The effects of NaOH-delignification, autohydrolysis and their combination at different severities were analyzed by determining the pore size distribution (DSC-thermoporometry), cellulose surface area and the accessible phenolic hydroxyls on lignin surface (adsorption of Congo Red and Azure B; ATR-FTIR) and crystallinity (WAXD). The correlation of these factors with initial and overall enzymatic hydrolyzability was studied and further put in order through principal component analysis. The major positive factors affecting hydrolyzability were cellulose surface area and accessibility of the pore system, while lignin content was the major negative factor accompanied by cellulose crystallinity. Autohydrolysis effectively increased the cellulose surface area by hemicellulose dissolution, but the high lignin content associated with small pores led to a lower hydrolyzability compared to delignified straw. Besides the removal of lignin, delignification led to a more accessible pore structure, which was supported by the remaining hemicellulose. Additionally, delignification increased the hydrophilicity of the remaining lignin, which also increased hydrolyzability. All pretreatments decreased cellulose crystallinity, which particularly increased the initial hydrolysis, but also improved the final carbohydrate conversion. The established weighed order of the factors behind enzymatic carbohydrate conversion is an important milestone in the path towards more efficient lignocellulosic sugar utilization in biorefineries.

Introduction

Production of fuels and chemicals from lignocellulosic raw materials has been widely studied in the recent years in pursuit of renewable alternatives to fossil sources. The common biotechnological approach relies on conversion of the lignocellulose carbohydrates to sugars by enzymatic hydrolysis with cellulases and thereafter to products by fermentation. Agricultural residues including straw, corn stover and bagasse, as well as forestry residues, have been subjected to vigorous research of pretreatments in order to facilitate hydrolysis and to establish an effective and economically feasible fractionation and conversion of carbohydrates to sugars.¹⁻⁵ The major pretreatment categories include delignification methods using alkali, solvents or oxidative agents, and acidic treatments at high temperatures using either dilute acid addition or autohydrolysis. Delignification methods generally lead to higher hydrolyzability and sugar yield compared to acidic methods^{1,5,6}, whereas autohydrolysis, catalysed by the acetic acid from the cleavage of hemicellulosic acetyls, does not require addition of chemicals.^{2,7,8} Although the biotechnological route to

lignocellulosic chemicals is not far from economic feasibility, the enzyme cost is still one of the major challenges.^{8,9}

The physical structure of lignocellulose consists of a network of cellulose fibril bundles, which are parallelly aligned in the secondary cell wall layers and less regular in the primary cell walls.¹⁰⁻¹² The cellulose fibril network is embedded in an amorphous matrix of hemicellulose and lignin. Hemicellulose binds to cellulose surfaces by hydrogen bonds, crosslinking the cellulose fibrils, but is also covalently linked to lignin.¹³⁻¹⁵ Lignin fills the remaining spaces, reduces water permeability and works as a physical barrier towards enzymes.^{16,17} The lignocellulose architecture is very recalcitrant towards enzymatic hydrolysis. A major hindrance is considered to be the non-productive binding of enzymes on lignin.¹⁸⁻²⁰ On the other hand, cellulose accessibility has been argued to play an even larger role in hydrolysis.^{4,21-23} The cellulose accessibility depends on the open cellulose surface area, as well as the porosity of the material. H. E. Grethlein²⁴ suggested that pore under the typical cellulase size of 5 nm are inaccessible and thereafter the pore diameters below 5 - 10 nm have been considered inaccessible in several studies.^{22,23,25} The determinants of accessibility and its role compared to lignin content remains under debate and conclusive understanding on the enzyme behavior within different materials has not been reached.

Pretreatments affect the structural features of lignocellulosics in different ways. Acidic pretreatments lead to the hydrolysis of hemicellulose, increasing the proportion of

^a Aalto University, School of Chemical Technology, P.O. BOX 16100, FI-00076 Espoo, Finland. email: ville.pihlajaniemi@aalto.fi.

^b University of Oulu, Fiber and Particle Engineering, P.O. Box 4300, FI-90014, Finland

† Electronic Supplementary Information (ESI) available.

See DOI: 10.1039/x0xx00000x

cellulose and lignin.^{2-4,8} Steam explosion is often used as the discharge method, which further degrades the material physically.^{4,26,27} The acidic pretreatments also lead to the dissolution of acids and phenolics that are inhibitory to cellulases, unless separated prior to hydrolysis, and also decrease the fermentability of the produced sugars. Delignification methods are based on dissolution and separation of lignin and varying proportions of hemicellulose, with the exception of ammonia fiber explosion (AFEX), in which the lignin is not separated from the solids.^{1,26,27} Both approaches generally increase porosity, pore area and cellulose area,^{4,22,23} and autohydrolysis decreases lignin area, while the opposite is observed for delignification.²⁸ While these properties generally correlate with hydrolyzability, the role of dissolution of different components has not been clearly assigned to these effects. Porosity has often been evaluated by solute exclusion methods which only give an impression of total porosity and average pore size,^{4,22,23} whereas the reports presenting continuous pore size distributions have not focused on the effects of pretreatments.^{25,29,30}

Another structural feature affecting hydrolysis is cellulose crystallinity. The amount of amorphous cellulose has been reported to correlate with the initial hydrolysis rate.^{17,32} However, the traditional view that the amorphous cellulose is hydrolyzed first, leading to increased crystallinity and thus higher recalcitrance, has been challenged since only small changes in crystallinity have been observed during the hydrolysis of lignocellulose materials.^{17,22,31,32} The crystallinity of cellulose is affected in different ways by pretreatments, being decreased by the disruption of crystal hydrogen bonding, and increased by degradation of amorphous cellulose. Most frequently, the degree of crystallinity has been defined as the crystalline index (Crl) of the total material obtained by X-ray diffraction.³³ However, the crystalline index has usually not been related to the actual cellulose content,^{21,25,34} which has led to some ambiguity in the perception of the effects of pretreatment to cellulose crystallinity.³⁵ Taking into account the changes in cellulose content, a decrease in cellulose crystallinity has been reported in correlation with pretreatment severity.^{3,36}

In order to evaluate the relative importance of the different structural changes to the hydrolyzability of lignocellulose materials, a systematic comparison across different pretreatments is required. Such reports are scarce,^{3,27} while most reports have focused on the analysis of either a single type of pretreatment or effect, and the relative importance of the factors has not been elucidated. Most studies have focused on either a single type of pretreatment or property to be analyzed. The pretreatments being compared have often been represented by single samples, providing no perspective on the dynamics of the properties with respect to treatment severity. We have recently studied in detail the effects of delignification, autohydrolysis and their combination on wheat straw, a major lignocellulosic agricultural residue, from the viewpoint of process sugar yields. In the current work we determine the effects of the pretreatments on the pore size distribution and area, cellulose and lignin area and crystallinity and their correlation to hydrolyzability of the pretreated solids. The

dissolution of hemicellulose and lignin are assigned to the changes in surface and pore properties, and the relative importance of the different factors on hydrolysis is statistically quantified, allowing elucidation of the major reasons behind hydrolyzability after each pretreatment.

Experimental

Pretreatments and enzymatic hydrolysis

Three different pretreatments were performed to wheat straw (Finland), including NaOH-delignification at NaOH-loadings of 3, 6 and 12% per straw dry matter (DM) at 140 °C for 1h and autohydrolysis at 185 – 195 °C for sufficient times to reach thermal severities (Log R₀) of 3.6, 3.8 and 4.0. In addition, a double treatment with NaOH delignification after autohydrolysis at Log R₀ 3.8 at NaOH-loadings of 3, 6 and 12% of original straw DM was carried out. The materials were washed and subjected to enzymatic hydrolysis at different dosages for 6 – 72 h. The washed solids were stored frozen and analyzed as such. The pretreatments, compositional analysis and enzymatic hydrolysis are described in detail in our previous work.⁵ Enzymatic hydrolysis was performed with commercial cellulases, supplemented with xylanase and cellobiase, at cellulase dosages of 4, 8 and 16 FPU g⁻¹ DM for 6 – 72 h. The hydrolysis yields at enzyme dosages corresponding to 8 and 20 FPU g⁻¹ glucan were interpolated from the data (see ESI for details) using the asymptotic model described previously.⁵

DSC thermoporometry

The pore size distribution (wet porosity) of the pretreated and washed solid samples was measured between diameters of 1.3 and 396 nm by DSC-thermoporometry, (tpDSC) adapted from Park *et al.*³⁰ with corrections to sample heat capacity as described by Driemeier *et al.*²⁹ Thermoporometry is based on the freezing point depression (ΔT) of water confined in pores, which depends on the pore diameter (x) according to the Gibbs-Thomson equation (Eq. 1), which assumes cylindrical pore geometry.

$$x = \frac{-2K_c}{\Delta T} \quad (1)$$

The factor K_c is a function of liquid properties and interfacial surface energies and the previously proposed value of 19.8 nmK was used in the present study.^{29,30} The materials were thoroughly wetted by submerging in deionized, degassed water for 24 h before preparing DSC-samples. Triplicate samples were analyzed with DSC 6000 (Perkin Elmer) in 50 μ L aluminum pans using the temperature program shown in ESI, table S3. The analysis consisted of stepwise heating of a frozen sample, and the amount of water melting in each step was calculated from the absorbed heat. The first step ($i = 0$) was used for determining the initial heat capacity of the sample (C_0), assuming no melting water. Similarly, the final step N provided the heat capacity of a molten sample and the step $N - 1$ allowed determination of the freezing free water outside the determined pores. The amount of melting water was divided by

ice density ($\rho_s = 917 \text{ g dm}^{-3}$) to obtain pore volume, which is usually presented as the cumulative pore volume as a function of pore diameter. The mass of melting water (M_i) in heating step i was calculated from the observed absorbed heat (Q_i) by subtracting the heat required for the temperature increase (δT_i) of the sample (Eq. 2).

$$M_i = \frac{Q_i - C_i * \delta T_i}{q_i} \quad (2)$$

The sample heat capacity (C_i) and enthalpy of ice melting (q_i) were calculated as described in detail previously,²⁹ where q_i depends on temperature and C_i accounts for the temperature dependence of specific heat capacities of ice and the sample solids, as well as the changing proportions of water and ice. The suggested temperature dependence of cellulose heat capacity ($0.0067 \text{ J g}^{-1}\text{K}^{-1}$) was used. As a reference, the pore size distribution of microcrystalline cellulose (MCC; Avicel PH101) was measured, showing a similar distribution as reported previously.²⁹ The pore area was calculated from the cumulative melting water based on Eq. 4, where the cumulative area in each discrete step is calculated separately from the definite integral of a linear correlation of ΔT and M with the slope of α_i (Eq. 5).

$$A = \sum_{i=1}^{N-2} \int_0^{M_i} \left(\frac{\alpha_i M_i + \Delta T_{i-1}}{K_c \rho_s} \right) dM \quad (3)$$

$$\alpha_i = \frac{\Delta T_i - \Delta T_{i-1}}{M_i} \quad (4)$$

Determination of the surface areas of cellulose and lignin by dye adsorption

Cellulose surface area was determined from the adsorption isotherm of the dye Congo Red (Direct red 28, Merck) adapting from Wiman *et al.*,⁴ and Inglesby and Zeronian³⁷. Of each material, 50 mg DM was weighed in 10 mL capped glass tubes, 4 mL of dye in pH 6 phosphate buffer (30 mM) was added and the tubes were incubated at 60 °C in a tilted position on a shaker at 200 rpm for 24 h. The tubes were then centrifuged and the supernatant filtered through a 0.45 μm PTFE-filter to remove particles. The unadsorbed Congo Red was determined spectrometrically at 498 nm. The isotherms were determined in duplicate at dye concentrations of 4, 2, 1, 0.25, 0.05 and 0 g L⁻¹. The parameters of the adsorption isotherm were fitted by non-linear regression (Matlab R2010b, Mathworks) to Brunauer Emmett Teller (BET) isotherm (for comparison to Langmuir isotherm, see ESI).³⁸ The BET-equation (Eq. 6) allows calculation of the monolayer adsorption maximum A_m from the detected adsorption A at equilibrium concentration c . The BET constant K was fitted separately for each isotherm, while the saturation concentration c_s was fitted as constant for all materials.

$$A = \frac{A_m K \frac{c}{c_s}}{\left(1 - \frac{c}{c_s}\right) \left((K-1) \frac{c}{c_s} + 1 \right)} \quad (5)$$

The cellulose surface area was calculated per DM from A_m with 1 g of dye representing the cellulose area of 1055 m².⁴

The lignin surface area was determined by adsorption of the dye Azure B. The method described in our laboratory was used, where reference data based on the Langmuir theory allows a single point determination, performed in duplicates at a dye concentration of 0.1 g L⁻¹ at pH 7 in 0.05 M Na-phosphate buffer.³⁹

Determination of cellulose crystallinity

The total crystallinity of the samples was analyzed using wide-angle X-ray diffraction (WAXD). Measurements were conducted on a Siemens D5000 diffractometer equipped with a Cu K α radiation source ($\lambda = 0.1542 \text{ nm}$). Samples were prepared by pressing tablets with a thickness of 1.5 mm from freeze-dried lignocellulose samples. Scans were taken over a 2θ (Bragg angle) range from 5° to 50° at a scanning speed of 0.1° s⁻¹ using a step time of 5 s (for diffractograms, see ESI). The degree of crystallinity in terms of the crystallinity index (CrI) was calculated from the peak intensity of the main crystalline plane (200) diffraction (I_{200}) at 22.2° and from the peak intensity at 18.0° associated with the amorphous fraction of cellulose (I_{am}) according to Eq. 6.³³ The samples 3 and 9 were analyzed as duplicates, showing 0.7% standard error from mean. Single analyses were carried out for the other samples.

$$CrI = \left(\frac{I_{200} - I_{am}}{I_{200}} \right) \quad (6)$$

ATR-FTIR analysis

Chemical properties of the solid material samples were analyzed with attenuated total reflection Fourier-transform infrared spectrometry. Prior to analysis, the samples were lyophilized, concealed in a miniature ball milling capsule, cooled in liquid nitrogen and milled for 2 min with (WigLBUG, USA). The samples were analyzed with Mattson 3000 FTIR spectrometer (Unicam) with a GladiATR unit (PIKE Technologies) and EZ Omnic software (Thermo Nicolet Corp.) with 64 scans at the wavenumber range of 400 - 4000 cm⁻¹ at a resolution of 2 cm⁻¹. The spectra were ATR- and baseline corrected and normalized. Microcrystalline cellulose (Avicel PH101) and alkaline extracted wheat straw lignin (GreenValue SA, Switzerland) were used as the reference materials.

Principal component regression

The importance of the effect of different factors in enzymatic hydrolyzability was quantified by principal component analysis (PCA) using Matlab R2010b (Mathworks). The principal components are linear combinations of the original variables, and more specifically, the eigenvectors of the covariance matrix of the variables. In principal component regression, the components that account for the majority of variance in the data are used as variables, to which the response is then linearly regressed.⁴⁰

The data was z-normalized and the variables X were transformed into principal components using *princomp*. The

first three components C , corresponding to 97% of total variance, were included in the PCA-model (for model prediction, see ESI, Figure S2). The hydrolysis data Y was regressed to C to obtain linear coefficients β_c , from which the linear coefficients corresponding to the original variables were derived as $\beta_x = C\beta_c$, describing the direction and magnitude of their effect.⁴⁰ A bootstrap distribution of the values was obtained by analyzing 1000 datasets of original size, resampled with replacement, from which the matrices with a rank lower than the number of variables (~15%) were excluded.⁴¹ The averages and standard deviations are reported. The relative accessibility of native straw was classified as an outlier resulting from effects outside the scope of this study, and was replaced by a linearly correlating value, for maintaining a full matrix. The correlation of the variable with hydrolysis was thus increased 0 – 6%.

Results and discussion

Effects of dissolution on porosity

Wheat straw was subjected to three pretreatments, each at three severities, including NaOH-delignification (3, 6 and 12% NaOH per DM), autohydrolysis [AH; severity factor (Log R0) 3.6, 3.8 and 4.0] and double treatment, where the straw autohydrolyzed at the severity of 3.8 was subjected to NaOH-delignification at the same NaOH dosages per native straw. The previously determined compositions of the materials are presented in Table 1.⁵ The NaOH-treatments dissolved up to 80% of lignin and minor proportions of hemicellulose, whereas autohydrolysis dissolved up to 60% of hemicellulose, while most of lignin remained in the solids and its proportion was slightly increased due to mass reduction. In each case the dissolution correlated with severity.

Table 1. Composition of the straw materials pretreated by NaOH-delignification, autohydrolysis and double treatment.

	Glucan	Xylan	Arabinan	Lignin*
Native straw	35%	21%	2%	23%
NaOH 3%	41%	23%	2%	20%
NaOH 6%	49%	24%	2%	14%
NaOH 12%	57%	26%	2%	8%
AH 3.6	44%	20%	1%	23%
AH 3.8	48%	17%	1%	24%
AH 4.0	51%	12%	0%	25%
Double 3%	58%	13%	0%	20%
Double 6%	65%	12%	0%	15%
Double 12%	74%	12%	0%	9%

*Including Klason- and acid soluble lignin

The effects of the dissolution of lignin and hemicellulose on the porosity of the materials were studied. The pore size distribution of each sample was determined within the pore diameter detection range of 1.3–396 nm, thus representing the porosity of the cell walls, while excluding the cell lumens, which

are typically tens of micrometers in diameter.^{11,42} The pore size distributions at different pretreatment severities can be assumed to represent different stages of dissolution. Native straw showed a total pore volume of 1060 $\mu\text{L g}^{-1}$ and a sharp upward turn in cumulative pore volume at 50 nm, above which the majority of pores resided. Already under the mildest conditions of NaOH- and AH-treatments (Fig. 1A & B), these larger pores were either collapsed or widened above the detection limit, and simultaneously smaller pores were formed. These may partly result from removal of extractives and loosening of the cell wall structure by elevated temperatures, allowing water to penetrate into the material.

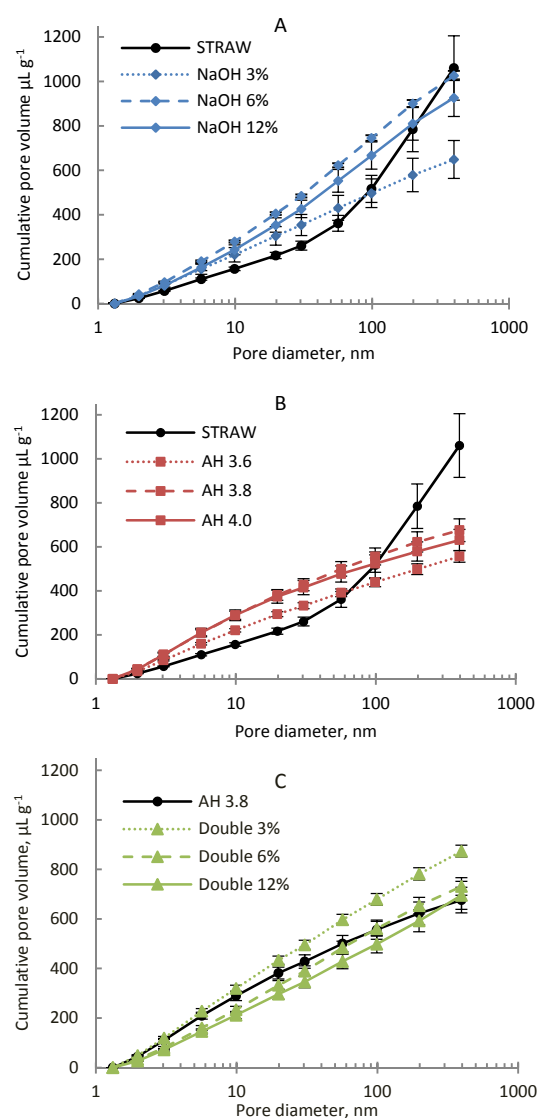


Fig. 1 Pore size distributions of straw before and after A) NaOH-delignification, B) autohydrolysis and C) their combination. Error bars represent the standard error of triplicate analysis.

Increasing the NaOH-dosage of delignification to 6% resulted in emergence of pores of all sizes leading to a total pore volume similar to native straw, whereas increasing autohydrolysis severity to 3.8 showed considerably lower increase in porosity reaching a total pore volume of 630 $\mu\text{L g}^{-1}$, and formation of pores of with a diameter below 20 nm. Further increase in

severity led to a decrease in porosity in both cases, suggesting widening of the existing pores taking over the formation of new ones. In the double treatment the lowest NaOH dosage (3%) led to the formation of relatively large pores up to a total volume of $870 \mu\text{L g}^{-1}$ (Fig. 1 C), but further increase in NaOH dosage caused decreasing porosity and a shift in the shape of the distribution curve from convex (upwards) towards concave, without ever reaching the porosity observed in direct NaOH-delignification.

The high porosities after NaOH-treatment were accompanied by the highest hemicellulose contents (Table 1), in accordance with previously reported results.²⁵ This supports the hypothesis of hemicellulose as a spacer and a crosslinker between fibril components.⁴³ When hemicellulose is retained, the dissolution of lignin leads to formation of a wide distribution of pores, while the cellulose network is still supported by hemicellulose. Different extents of hemicellulose removal showed only small differences in porosity, and subsequent lignin removal quickly led to porosity decrease. Hemicellulose dissolution is associated with the formation of relatively small pores, suggesting uniform dissolution deep within the material, while lignin dissolution leads to more bulky removal of material, and in the absence of hemicellulose, to removal of the smaller pores. Pretreatments have generally been shown to increase lignocellulose porosity^{4,23} whereas drying leads to pore collapse.³⁰

Peculyte *et al.*²² recently discussed the morphology of lignin-free materials, comprising a network of fibril bundles. The pore diameter defined in the tpDSC-analysis represents the diameter of the respective ice crystal formed in a confined space.²⁹ While cylindrical pore geometry is a decent simplification in fibril networks embedded in amorphous non-cellulosic constituents, in a completely delignified material the diameter may rather represent the distance between the fibril bundles of the network. The exclusion of pores above 396 nm from analysis leads to exclusion of no more than 6 - 12% of pore surface area, according to extrapolation of the pore size distributions to account for the water outside the determined pores. This is in accordance with previous estimates of the interior pore surface accounting for over 90% of total surface area.⁴⁴ This signifies the importance of measuring the area that includes the pore surfaces, rather than only the external particle surfaces.

Surface properties of pretreated straw

The surface areas (SA) of cellulose and lignin were determined by dye adsorption and the total pore area was calculated from the pore size distributions. Cellulose surface area increased as a function of severity in each pretreatment (Fig. 2A). NaOH- and AH treatments showed cellulose areas up to $150 \text{ m}^2 \text{ g}^{-1}$ and the highest area of $163 \text{ m}^2 \text{ g}^{-1}$ was reached by the double treatment. Rather than the total cellulose area, the specific surface area (SSA), calculated per cellulose content, better describes the changes in cellulose properties. The specific surface area of cellulose correlated with autohydrolysis severity and thus with hemicellulose dissolution, while the NaOH-treatment resulted only in a small increase and the double treatment actually

decreased the specific cellulose area (Fig. 2B). This seems to reflect the closer contact of cellulose with hemicellulose rather than with lignin,¹³ whereas severe delignification reactions may lead to lignin condensation on the revealed cellulose surfaces. Accordingly, in a previously reported acidic steam pretreatment (SO_2) of softwood, where hemicellulose was almost completely removed already at the lowest severity, no correlation of cellulose surface area with further severity increase was observed.⁴

Lignin surface area was determined using the dye Azure B, which binds to the phenolic hydroxyl groups of lignin, thus representing the surface accessible phenolic hydroxyls more precisely than the physical area.³⁹ Despite the lignin removal by NaOH-treatments, the total lignin area was only slightly decreased by direct delignification and increased by the double treatment, indicating increase of the specific surface area of lignin (Fig. 2C) as a function of NaOH-dosage. This may result from a thin residual or recondensed lignin layer, in combination with increased phenolic hydroxyl content due to alkaline

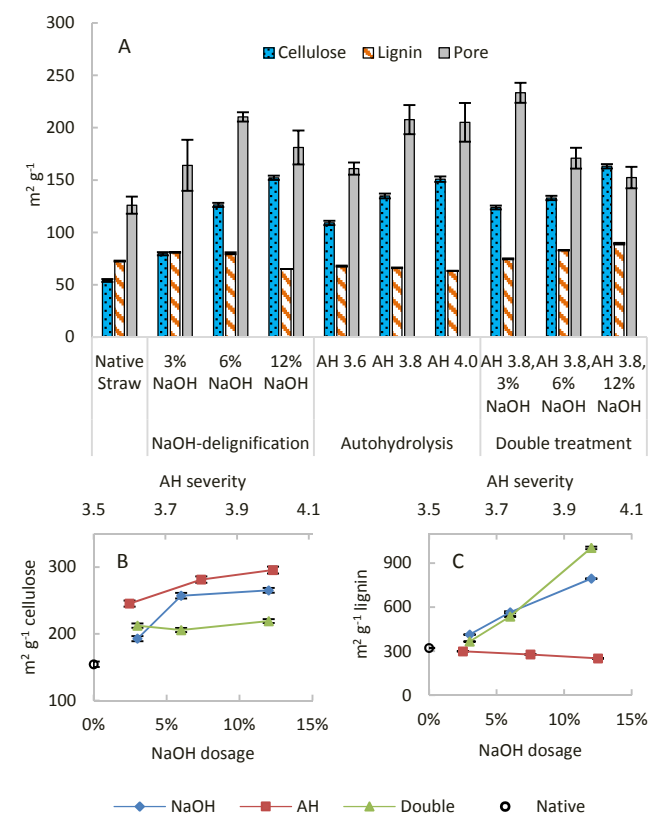


Fig. 2 Surface areas, (A) and specific surface areas of cellulose (B) and lignin (C) in pretreated straw. The error bars represent standard error.

degradation of the aryl-ether bonds in lignin.⁴⁵ The increase in lignin SSA may thus indicate the change in the chemical surface properties of the remaining lignin and consequent increase in lignin hydrophilicity. In contrast to the NaOH-treatments, autohydrolysis caused a small decrease in the specific lignin area as a function of severity. While autohydrolysis does not substantially remove lignin, it leads to partial translocation of lignin into spherical deposits,⁴⁶ which may partly explain reduction in specific surface area. It has also

been suggested that acidic treatments increase lignin hydrophobicity.¹⁹ These trends in lignin area changes are in accordance with our previous study of autohydrolysis and subsequent aqueous ammonia treatment.²⁸

Being cationic, Azure B also binds to negatively charged carboxylic acid groups, which may be formed in oxidative degradation of lignin and cellulose. In order to rule out such non-specific binding, the materials were analyzed with ATR-FTIR. Unconjugated carbonyl groups show a characteristic band between 1705 and 1730 cm^{-1} .^{47,48} Such band was present in native straw and was removed by the NaOH-treatments (Fig. 3 A & C). Although it is difficult to determine whether the carbonyl band results from carboxylic acids or other carbonyl compounds, it is clear that the carbonyl content did not correlate with Azure B adsorption. This suggests that new carboxylic groups were not formed and supports the interpretation of the Azure B signal as a measure of phenolic hydroxyls on the lignin surface. The removal of the band with NaOH-treatments and the lowest severity autohydrolysis (Fig. 3B) represents the cleavage of ester linkages of hemicellulosic acetyls and hydroxycinnamates,¹⁵ in accordance with its previous assignment as the "hemicellulose band".⁴² However, at a higher severity of autohydrolysis (3.8), the carbonyl band reappeared (Fig. 3B) and this time a higher NaOH-dosage was required for its subsequent removal (Fig. 3C). A similar reappearing carbonyl band was previously assigned to unconjugated aliphatic ketones in lignin side chains⁴⁹ formed by acidic degradation of the β -O-4 bonds,⁵⁰ whereas alkaline degradation rather leads to the formation of hydroxyl groups.⁴⁵ The lignin-specific aromatic bands at 1510 and 1460 cm^{-1} indicate the removal of lignin by NaOH-treatments and a slight increase in its content by autohydrolysis. The increase in lignin content may partly result from the formation of pseudo-lignin, a condensation product of lignin and carbohydrate degradation products, formed under acidic conditions.^{49,50}

The total pore area was increased by the pretreatments compared to native straw, but increasing NaOH dosage eventually led to downturn in pore area, as well as in pore volume, as described above. The highest pore area (93 $\text{m}^2 \text{g}^{-1}$), resulting from the high proportion of small pores remaining after the preceding autohydrolysis (see above) was obtained by the double treatment at 3% NaOH-dosage. It is acknowledged that the determination of the total pore area relies on the assumption of cylindrical pore geometry, which may somewhat underestimate the area of rough surfaces and overestimate the area of a fibril network morphology, where no continuous pore walls exist.

Cellulose crystallinity

Cellulose crystallinity is affected by pretreatments in different ways. While the treatment may open the crystal hydrogen bonding and increase amorphous regions, the amorphous cellulose may also be specifically degraded, particularly under acidic conditions.^{22,27} For determining the effect of the current pretreatments, the crystallinity index (CrI), which indicates the total crystallinity in the material, was

determined by WAXD. The CrI was increased from 0.49 up to 0.59 - 0.63 by the pretreatments (Table 2).

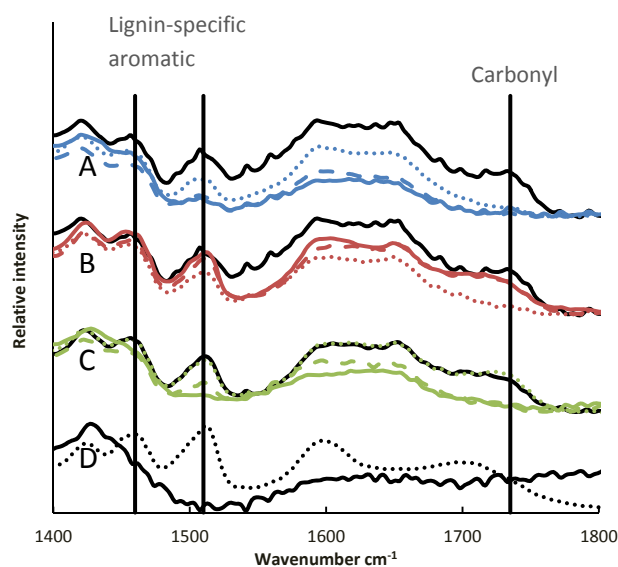


Fig. 3 The FTIR-spectra of A) straw (black) in NaOH-treatment (blue), B) straw (black) in autohydrolysis (red) and C) AH-straw (Log R₀ 3.8; black) in double treatment (green). Dotted, dashed and solid lines represent the order of increasing treatment severity (3, 6 and 12% NaOH dosage or Log R₀ 3.6, 3.8 and 4.0 in autohydrolysis). D) Reference materials MCC (Avicel PH101, solid line) and Green Value straw lignin (dotted).

However, the ratio of CrI to the cellulose content showed an opposite trend, decreasing to 1.03 by NaOH-treatment, 1.24 by autohydrolysis and 0.81 by double treatment, compared to the initial 1.38. This suggests that while the total amount of crystallinity is increased due to the increased cellulose content, the crystallinity of cellulose itself is decreased, which is in accordance with previously reported considerations.^{3,34,36} It should be noted that it may not be straightforward to relate CrI to cellulose, because hemicellulosic glucose increases the apparent cellulose content and the commonly applied peak height method for CrI-determination by X-ray diffraction slightly overestimates crystallinity.^{31,33,36} In the current study, however, the amount of glucose dissolved by NaOH-treatment and autohydrolysis was small and did not correlate with xylose

Table 2. Crystallinity index (CrI) of the total material and the CrI/cellulose ratio.

	CrI	CrI / Cellulose
Native straw	0.49	1.38
NaOH 3%	0.52	1.27
NaOH 6%	0.58	1.17
NaOH 12%	0.59	1.03
AH 3.6	0.58	1.31
AH 3.8	0.59	1.24
AH 4.0	0.63	1.24
Double 3%	0.61	1.04
Double 6%	0.63	0.98
Double 12%	0.60	0.81

dissolution, suggesting that the CrI / cellulose ratio is a valid relative measure of the effects of the pretreatments on the crystallinity of cellulose itself. Alkaline treatment facilitated decrystallization more efficiently compared to autohydrolysis,

indicating that NaOH caused physicochemical effects that were more effective compared to the acidic treatment at a higher temperature. The crystallographs did not suggest particular differences between the crystal structures after different pretreatments (see ESI, Fig. S4).

Correlations to hydrolysis

For resolving the factors behind hydrolysability of the pretreated solids, its correlations with the determined physicochemical properties were studied (Fig. 4). The solids were washed in order to remove soluble sugars and inhibitors. The hydrolysis was studied at two different stages, including the initial glucan conversion (6 h, 8 FPU g⁻¹ glucan) and final carbohydrate conversion (72 h, 20 FPU g⁻¹ glucan), based on the previously reported hydrolysis results.⁵ Since several factors were correlated to hydrolysis, correlation between the factors themselves was also observed. Due to the correlated factors, linear regression could not be reliably used for the estimation of variable importance (for details, see ESI, Table S2). In order to elucidate the relative order of the factors despite the partial collinearity, principal component regression was applied.⁴⁰

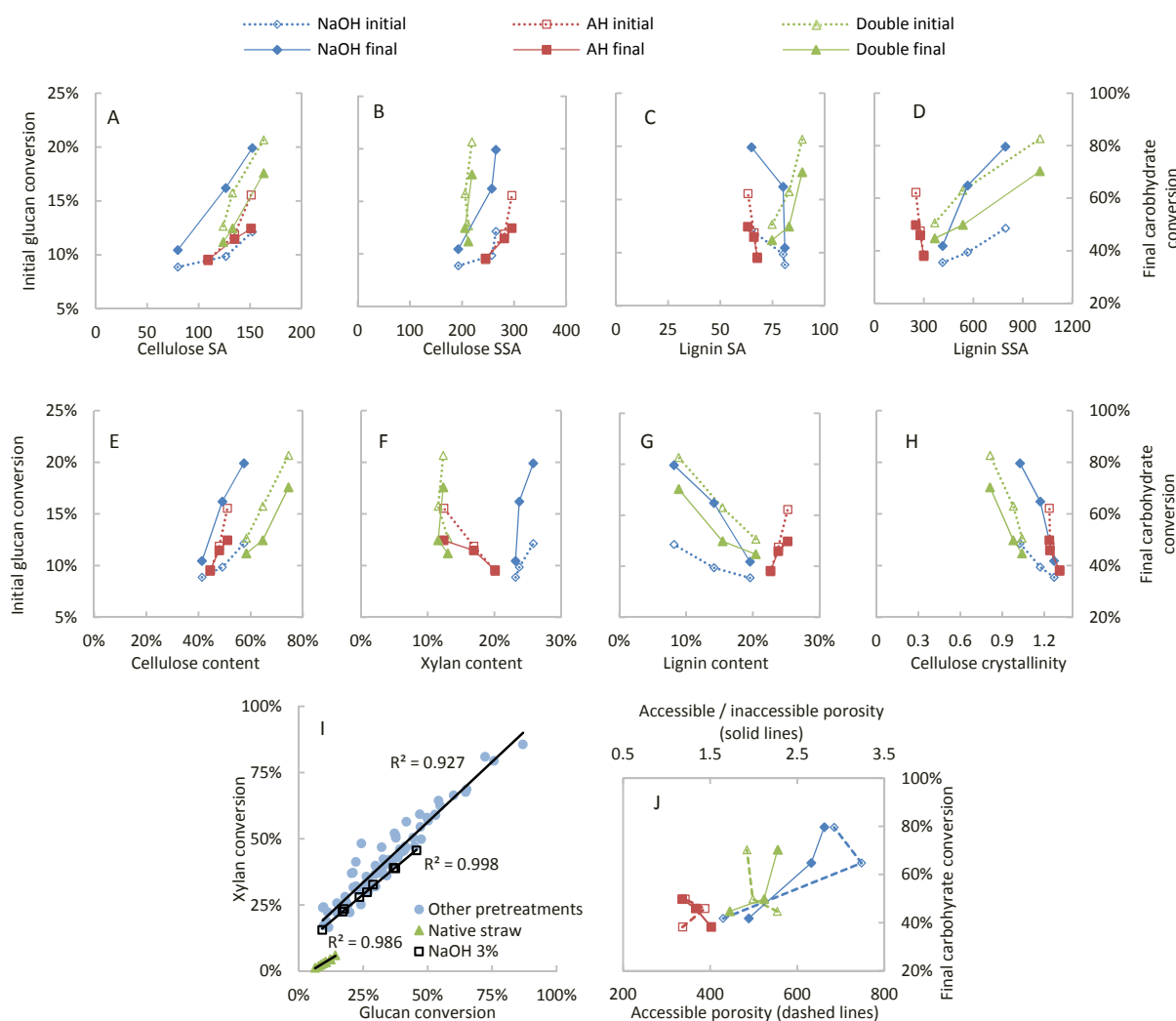


Fig. 4 Correlation of different factors to hydrolyzability with NaOH-delignified (blue diamonds), autohydrolyzed (red squares) and double treated (green triangles) straw. Initial glucan conversion with 8 FPU per g glucan for 6 h (A-H, dotted lines, open markers, left axis) and final carbohydrate conversion with 20 FPU per g glucan for 72 h (A-H, solid lines, filled markers, right axis). Surface area (SA) is given as $\text{m}^2 \text{g}^{-1}$ DM and specific surface (SSA) area as $\text{m}^2 \text{g}^{-1}$ of the corresponding material. I: correlation of the glucan conversion to xylan conversion. J: correlation of accessible pore volume (dashed lines) and the ratio of accessible and inaccessible pore volume to final carbohydrate conversion.

Table 3. The linear coefficients β and corresponding standard deviations SD of for initial glucan conversion and final carbohydrate conversion according to the PCA-model.

Variable	Initial glucan conversion		Final carbohydrate conversion	
	β_I	SD	β_F	SD
Cellulose SSA	0.18	0.17	0.41	0.12
Lignin / Cellulose	-0.18	0.05	-0.24	0.05
Lignin SSA	0.11	0.12	0.22	0.14
Xylan / Cellulose	-0.42	0.12	0.06	0.06
Rel. Accessibility	-0.14	0.09	0.33	0.08
CrI / cellulose	-0.33	0.06	-0.15	0.04

Cellulose SSA, the ratio of lignin and xylan contents to cellulose and CrI / cellulose ratio were included in the PCA-model, all in relation to the cellulose content and hence to the enzyme dosage, thus portraying their contributions towards standardized cellulose hydrolysis. Lignin SSA and relative accessibility were included as such as relative measures of material properties. The linear coefficients derived from the PCA-model (β) represent the direction and standardized magnitude of the effects (Table 3).

The most pronounced positive factor was the cellulose surface area (Fig. 4 A & B), showing unanimous correlation with hydrolyzability with all pretreatments, and the largest effect ($\beta_F = 0.41$) for final carbohydrate conversion. This highlights the importance of the removal of physical barriers and the kinetic role of the cellulose surface representing the available substrate amount in the reaction. Hemicellulose has been considered to be one of the barriers for hydrolysis.^{4,17} Initial glucan conversion was indeed slowed down by hemicellulose, which was particularly visible for NaOH delignified straw (Fig. 4F). Although hemicellulose was the most important factor for initial glucan conversion ($\beta_I = -0.42$), it had practically no effect on the final carbohydrate conversion, since it was efficiently hydrolyzed and comprised a significant part of the sugar yield. According to extensive amount of previous hydrolysis data,⁵ the xylan conversion correlated linearly with glucan conversion (Fig. 4I) at a constant ratio, which was the lowest for the mildest NaOH-delignification and native straw (shown separately). The low ratios corresponded to the lowest degree of deacetylation, which suggests that some ester crosslinks between hemicellulose and lignin might have remained.^{5,15} Nevertheless, the esters are cleaved at relatively mild conditions, after which the hydrolysis of cellulose and hemicellulose proceed hand in hand, regardless of their relative proportions, enzyme dosage, hydrolysis time or pretreatment.^{5,15,49}

Lignin content had the highest negative effect on final conversion ($\beta_F = -0.24$) and showed a generally negative correlation with hydrolysis (Fig. 4G). The lignin SA, however,

showed little correlation (Fig. 4C) and lignin SSA, in fact, correlated positively with hydrolysis (Fig. 4D), the latter being the third positive factor ($\beta_F = 0.33$). The observed lignin area corresponds to the accessible phenolic hydroxyls of the surface, the concentration of which is increased by lignin degradation, apparently resulting in more efficient hydrolysis. This fits the hypothesis of hydrophobic interactions being the major mechanism of non-productive binding of cellulases.¹⁸ It is also in agreement with the report suggesting that cellulase binding is reduced by negative charges on lignin.²⁰ Increased lignin hydrophilicity may therefore be the reason for the observed positive effect, implying that surface modification of lignin could prove beneficial. Surfactants have been shown to decrease non-productive binding, but chemical modifications could also be considered.⁵¹

While the effect of cellulose crystallinity is a debated subject, the current results unanimously indicate that a decrease in crystallinity increases both initial and final hydrolysis (Fig. 4H). It is the second largest factor ($\beta_I = -0.33$), affecting initial hydrolysis, consistent with the expectation of rapid hydrolysis of the amorphous regions.³² The effect on final conversion is smaller ($\beta_F = -0.15$), being the smallest factor after xylan content, signifying that the hydrolysis rate of the crystalline regions is more relevant to the outcome compared to the amorphous fraction. Nevertheless, the decrease of crystallinity may be accompanied by increased crystal dislocations, increasing accessibility to endoglucanases and thus allowing crystal decomposition at a higher rate.

Pores under 5 - 10 nm in diameter are often considered inaccessible by cellulases.²²⁻²⁵ In the current study, the pore area and volume termed accessible in this manner (over 10 nm) both showed a similar, generally slightly positive correlation with final conversion (shown for volume, Fig. 4J, dotted lines). However, for each pretreatment separately, the correlation was less clear. More consistent trends were shown by the ratio of accessible and inaccessible pore volume, termed relative accessibility, which captures a broader effect of pore widening by dissolution, compared to a sharp physical cut-off (Fig. 4J, solid lines). The relative accessibility turned out to be the second largest factor for final conversion ($\beta_F = 0.33$), thus having a larger effect compared to lignin. For the initial glucan conversion, the relative accessibility showed no correlation (not shown) and even showed a small negative effect ($\beta_I = -0.14$), suggesting that the rapid initial hydrolysis takes place at the easily accessible surfaces and amorphous regions. However, the contribution of less accessible regions to the final hydrolysis outcome is significant and the pore structure seems to play a crucial role. Consistently, the effect of the AFEX-treatment has been attributed to the increased porosity, although lignin is not removed from the solids.²⁶ While the smallest pores may eventually be revealed by degradative events, many factors may restrict hydrolysis within pores. In smaller pores the probability is higher for only a short piece of the cellulose chain

to be continuously exposed, being restricted by lignin, hemicellulose, a crossing cellulose fibril or simply by not being aligned with the accessible enzyme route. This will limit the productivity of a single processive hydrolysis run to a small number of glucose units, and increase the risk of running into non-productive interaction with lignin within the pore.

The physical effects of the pretreatments are illustrated in Fig. 5. The NaOH-treatment efficiently removes lignin, greatly

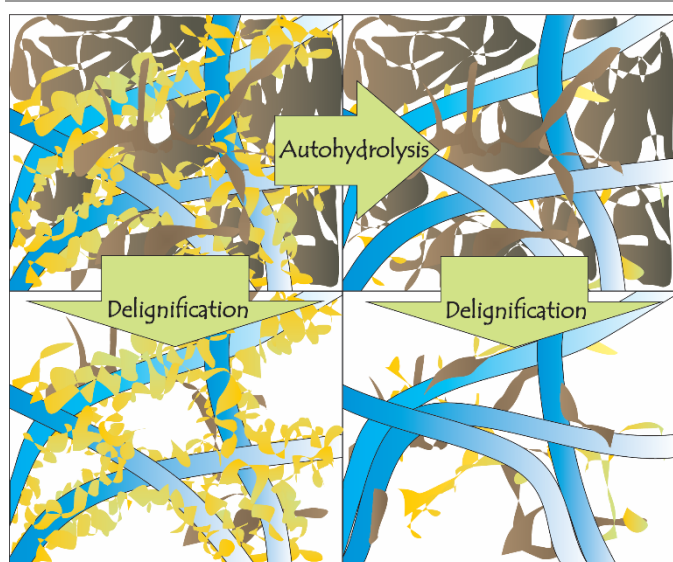


Fig. 5 Physical effects of pretreatments. Native lignocellulose (top left), with cellulose fibrils (blue) embedded in a matrix of hemicellulose (yellow) and lignin (brown). Delignification reveals large pores, while the hemicellulose supports the fibril network. Autohydrolysis reveals cellulose surface, but accessibility is limited by lignin. Subsequent delignification leads to collapse of the network structure.

enhances accessibility of the pore system and increases the hydrophilicity of the remaining lignin, leading to superior hydrolyzability. The double treatment resulted in the lowest lignin content and cellulose crystallinity, which contributed to the highest initial glucan conversion, but the final conversion appeared to be suppressed by constrained accessibility due to the absence of hemicellulose. Autohydrolysis opposed the general trends of hydrolyzability with respect to lignin content and area and relative accessibility, due to increased proportion of lignin and small differences in pore size distribution. These effects were overcome by the efficient uncovering of cellulose surface by hemicellulose dissolution, which appeared to be the major effect behind hydrolyzability of autohydrolyzed straw. Nevertheless, lower hydrolyzability was achieved compared to the delignification methods. Apparently the high lignin content leads to non-productive binding of enzymes, which is most likely intensified by the narrow pores, eventually suppressing hydrolysis.

Conclusions

Enzymatic hydrolysis of lignocellulose faces some particular constraints compared to chemically catalyzed hydrolysis. Uncovering cellulose surface was found to be the most important contributor to hydrolysis. Nevertheless, retaining

some of the hemicellulose associated with cellulose is beneficial since it maintains an accessible pore structure in the fibril network, before it is eventually hydrolyzed. Therefore the most beneficial aims in terms of hydrolyzability seem to be the removal of lignin and increasing its hydrophilicity, which are achieved by alkaline delignification. Autohydrolysis was superior in revealing cellulose surface, but a high lignin content together with restricted pore accessibility appeared to pose an inherent restriction to conversion yields. Surface modification of lignin towards increased hydrophilicity could improve the performance of autohydrolyzed straw, but its subsequent delignification offers no extra benefit compared to direct delignification, since it suffers from decreased accessibility due to the lack of hemicellulose. Decreasing cellulose crystallinity was beneficial but not crucial for hydrolysis.

While this study focused on the hydrolyzability of the pretreated solids, it should be noted that the hemicellulosic sugar fraction from autohydrolysis contains inhibitors that reduce the fermentability of the produced sugars, which are virtually absent in the hydrolysates from delignified materials. The higher carbohydrate content after delignification may also allow a higher volumetric productivity in hydrolysis processes with high solids loadings. While autohydrolysis is a simple process with no chemical additions, delignification offers a higher yield potential with less inhibitors, and the choice thus depends on the availability and the cost of the alkaline chemical recovery process. Our results suggest that the autohydrolysis process may benefit from further research in lignin surface modification with a minimal chemical consumption.

Acknowledgements

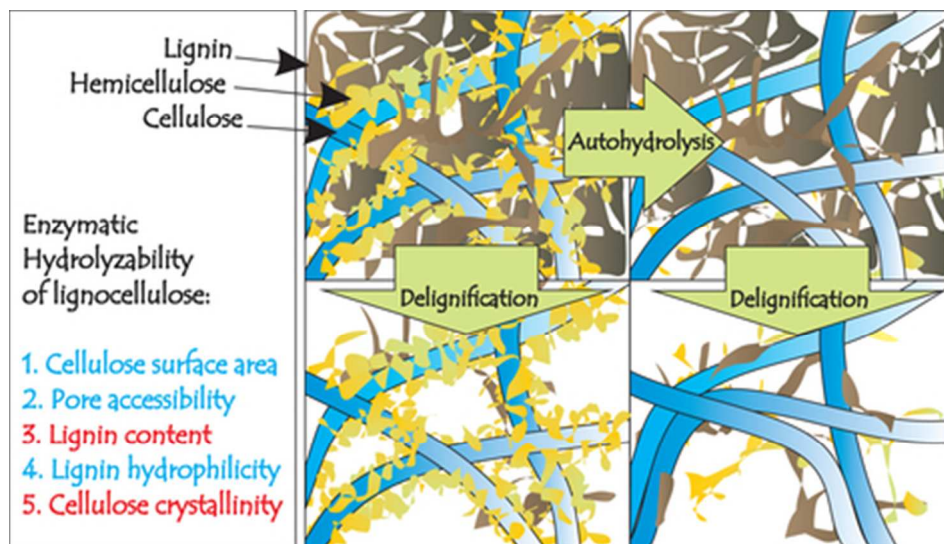
We acknowledge the Neste Oil Corporation and the Finnish Funding Agency for Technology and Innovation (Microbial Oil Project) for funding. Additionally, this work was partly funded by the Fortum Foundation. We express gratitude to Kuisma Littunen for FTIR expertise. This work is dedicated to celebrate Professor Emeritus Simo Laakso's career of scientific leadership.

References

- 1 Y. Chen, M. A. Stevens, J., Y. Zhu, J. Holmes and H. Xu, *Biotechnol. Biofuels*, 2013, **6**, 8.
- 2 M. Ø. Petersen, J. Larsen and M. H. Thomsen, *Biomass Bioenergy*, 2009, **33**, 834–840.
- 3 S. Singh, G. Cheng, N. Sathitsuksanoh, D. Wu, P. Varanasi, A. George, V. Balan, Gao, X., R. Kumar, B. E. Dale, C. E. Wyman, B. E. Simmons, *Front. Energy Res.*, **2**, 2015, 62.
- 4 M. Wiman, D. Dienes, M. A. T. Hansen, T. van der Meulen, G. Zacchi, G. Lidén, *Bioresour. Tech.*, 2012, **126**, 208–215.
- 5 V. Pihlajaniemi, M. H. Sipponen, O. Pastinen, I. Lehtomäki, S. Laakso, *Green Chem.* 2015, **17**, 1683–1691.
- 6 O. Sánchez, R. Sierra and C. J. Alméciga-Díaz, in *Alternative Fuel*, ed. M. Manzanera, InTech, 2011, ch. 6 pp. 111–154.
- 7 A.T.W.M Hendriks, G. Zeeman, *Biores. Technol.*, 2009, **100**, 10–18.

- 8 J. Larsen, M. Ø. Haven, L. Thirup, *Biomass Bioenergy*, **46**, 2012, 36-45.
- 9 D. Klein-Marcuschamer, P. Oleskowicz-Popiel, B. A. Simmons, *Biotechnol. Bioeng.*, **109**, 2012, 1083-1087.
- 10 I. Duchesne, G. Daniel, *Nord. Pulp Pap. Res. J.*, 2000, **15**, 54-61.
- 11 S.-Y. Ding, Y.-S. Liu, Y. Zeng, M. E. Himmel, J. O. Baker, E. A. Bayer, *Science*, 2012, **338**, 1055-1060.
- 12 S.-Y. Ding, S. Zhao, Y. Zeng, *Cellulose*, 2014, **21**, 863-871.
- 13 H. V. Scheller, P. Ulvskov, *Annu. Rev. Plant Biol.*, 2010, **61**, 263-289.
- 14 J. Gu, J. M. Catchmark, *Cellulose*, 2013, **20**, 1613-1627.
- 15 X. Chen, J. Shekiri, M. A. Franden, W. Wang, M. Zhang, E. Kuhn, D. K. Johnson and M. P. Tucker, *Biotechnol. Biofuels*, 2012, **5**, 8.
- 16 L. T. Fan, M. M. Gharpuray and Y.-H. Lee, in *Cellulose Hydrolysis*, Springer-Verlag, 1987, ch 3, pp. 21-120.
- 17 X. Zhao, L. Zhang, D. Liu, *Biofuels, Bioprod. Biorefin.*, 2012, **6**, 465-482.
- 18 H. Palonen, F. Tjerneld, G. Zacchi, M. Tenkanen, *J. Biotechnol.*, 2003, **107**, 65-72.
- 19 S. Nakagame, R. P. Chandra, J. F. Kadla, J. N. Saddler, *Bioresour. Technol.*, 2011, **102**, 4507-4517.
- 20 J. L. Rahikainen, J. D. Evans, S. Mikander, A. Kalliola, T. Puranen, T. Tamminen, K. Marjamaa and K. Kruus, *Enzyme Microb. Technol.*, 2013, **53**, 215-321.
- 21 J. A. Rollin, Z. Zhu, N. Sathitsuksanoh, Y.-H. P. Zhang, *Biotechnol. Bioeng.*, 2011, **108**, 22-30.
- 22 A. Peculyte, K. Kalström, P. T. Larsson, L. Olsson, *Biotechnol. Biofuels*, 2015, **8**, 56.
- 23 X. Meng, M. Foston, J. Leisen, J. DeMartini, C. E. Wyman, A. J. Ragauskas, *Bioresour. Technol.*, 2013, **144**, 467-476.
- 24 H. E. Grethlein, *Nat. Biotechnol.*, 1985, **3**, 155-160.
- 25 J. Bragatto, F. Segato, J. Cota, D. B. Mello, M. M. Oliveira, M. S. Buckeridge, F. M. Squina, C. Driemeier, *J. Phy. Chem.*, 2012, **116**, 6128-6136.
- 26 S. P. S. Chundawat, B. S. Donohoe, L. da Costa Sousa, T. Eider, U. P. Agrawal, F. Lu, J. Ralph, M. E. Himmel, V. Balan, B. E. Dale, *Energy Environ. Sci.*, **4**, 2011, 973-984.
- 27 R. Kumar, G. Mago, V. Balan, C. E. Wyman, *Bioresour. Technol.*, **100**, 2009, 3948-3962.
- 28 M. H. Sipponen, V. Pihlajaniemi, O. Pastinen, S. Laakso, *RSC Adv.*, 2014, **4**, 36591-36596.
- 29 C. Driemeier, F. M. Mendes, M. M. Oliveira, *Cellulose*, **19**, 1051-1063.
- 30 S. Park, R. A. Venditti, H. Jameel, J. J. Pawlak, *Carbohydr. Polym.*, 2006, **66**, 97-103.
- 31 S. Park, J. O. Baker, M. E. Himmel, P. A. Parilla, D. K. Johnson, *Biotechnol. Biofuels*, 2010, **3**, 10.
- 32 M. Hall, P. Bansal, J. H. Lee, M. J. Realff, A. S. Bommaris, *FEBS J.*, 2010, **277**, 1571-1582.
- 33 L. Segal, J. J. Creely, A. E. Jr Martin, C. M. Conrad, *Text. Res. J.* 1959, **29**, 786-794.
- 34 T. H. Kim, J. S. Kim, C. Sunwoo, Y. Y. Lee, *Bioresour. Technol.*, 2003, **90**, 39-47.
- 35 Y. Pu, F. Hu, F. Huang, B. H. Davison, A. J. Ragauskas, *Biotechnol. Biofuels*, 2013, **6**, 15.
- 36 C. Driemeier, M. T. B. Pimenta, G. J. M. Rocha, M. M. Oliveira, D. B. Mello, P. Maziero, A. R. Goncalves, *Cellulose*, 2011, **18**, 1509-1519.
- 37 M. K. Inglesby, S. H. Zeronian, *Cellulose*, 2002, **9**, 19-29.
- 38 S. Brunauer, P. H. Emmett, E. Teller, *J. Am. Chem. Soc.*, 1938, **60**, 309-319.
- 39 M. H. Sipponen, V. Pihlajaniemi, K. Littunen, O. Pastinen, S. Laakso, *Bioresour. Technol.*, **169**, 80-87.
- 40 R. X. Liu, J. Kuang, Q. Gong, X. L. Hou, *Comput. Methods. Programs. Biomed.*, 2002, **71**, 141-147.
- 41 S. Tonidandel, J. M. LeBreton, J. W. Johnson, *Psychol. Methods*, 2009, **14**, 387-399.
- 42 R. Liu, H. Yu, Y. Huang, *Cellulose*, 2005, **12**, 25-34.
- 43 D. S. Thompson, *J. Exp. Bot.*, 2005, **56**, 2275-2285.
- 44 Q. Q. Wang, Z. He, Z. Zhu, Y.-H. P. Zhang, Y. Ni, X. L. Luo, J. Y. Zhu, *Biotechnol. Bioeng.*, 2012, **109**, 381-389.
- 45 J. Lora in *Monomers, Polymers and Composites from Renewable Resources*, ed. M. N. Belgacem and A. Gandini, Elsevier, 1st edn, 2008, ch. 10, 241-225.
- 46 M. J. Selig, S. Viamajala, S. R. Decker, M. P. Tucker, M. E. Himmel, T. B. Vinzant, *Biotechnol. Prog.*, 2007, **23**, 1333-1339.
- 47 O. Faix, in *Methods in Lignin Chemistry*, ed. S. Y. Lin, C. W. Dence, Springer, Berlin, 1992, 4.1, 83-109.
- 48 C. G. Boeriu, D. Bravo, R. J. A. Gosselink, J. E. G. van Dam, *Ind. Crops Prod.*, 2004, **20**, 205-218.
- 49 P. Sannigrahi, D. H. Kim, S. Jung, A. Ragauskas, *Energy Environ. Sci.*, 2011, **4**, 1306-1310.
- 50 R. B. Santos, P. W. Hart, H. Jameel, H.-m. Chang, *Bioresources*, 2013, **8**, 1456-1477.
- 51 B. Sipos, M. Szilágyi, Z. Sebestyén, R. Perazzini, D. Dienes, E. Jakab, C. Crestini, K. Réczey, *C. R. Biologies*, 2011, **334**, 812-823.

Applying an elaborate set of pretreatments, the effects of lignocellulose properties on enzymatic hydrolyzability were arranged in the order of importance.



40x22mm (300 x 300 DPI)